Birefringence and strain-induced crystallization for stretched cellulose acetate propionate films

Shogo Nobukawa[*†]*, Akichika Nakao, Songsurang Kultida, Panitha Pulkerd, Hikaru Shimada, and Masayuki Yamaguchi*[*]

Japan Advanced Institute of Science and Technology, 1-1 Asahidai, Nomi, Ishikawa 923-1292, Japan

*Corresponding authors: nobukawa@nitech.ac.jp (S. N.), m_yama@jaist.ac.jp (M. Y.)

† Present address (S.N.):

Department of Life Science and Applied Chemistry, Nagoya Institute of Technology, Gokiso-cho, Showa-ku, Nagoya, Aichi 466-8555, JAPAN

Title running head: Birefringence and stretched induced crystallization for stretched CAP films

ABSTRACT

We investigated wavelength dependence of birefringence (Δn) for cellulose acetate propionate (CAP) films stretched at various draw ratios (DRs) and strain rates (SRs), by comparing the result of cellulose triacetate (CTA). CAP exhibited an extraordinary wavelength dispersion of Δn although CTA showed an ordinary dispersion, indicating that Δn of CAP is determined by acetyl and propionyl groups. The extraordinary dispersion for CAP became stronger at larger DR and higher SR. The thermal analysis data suggested that the hot-stretching induces the crystallization of CAP and the crystal size increases with increasing DR and SR. Furthermore, two-dimensional X-ray diffraction pattern of CAP exhibited the orientation of the induced crystal as well as that of CTA, which is one of semi-crystalline polymers. These results mean that the acetyl orientation in CAP becomes stronger than the propionyl orientation. This conclusion is reasonable because acetyl group is more tightly confined to a pyranose ring than propionyl.

Keywords: birefringence ; wavelength dependence ; strain-induced crystallization

INTRODUCTION

When polymer films are stretched beyond a glass transition temperature (T_g), birefringence, Δn, is generated by the chain orientation.[1] Here, Δn is defined as a difference of two refractive indices, $n_{//}$ and $n_{\perp}$ in the directions parallel and perpendicular to the stretching direction.

$$\Delta n = n_{//} - n_{\perp} \tag{1}$$

For most of amorphous polymers, Δn is proportional to a tensile stress, σ, since the two properties are associated with the orientation of the chain segment.[1]

$$\Delta n = C\sigma \tag{2}$$

Here, C is the stress-optical coefficient, which is determined from repeating units of polymers. This relation is called the stress-optical rule (SOR). Since Δn is related to polarizability anisotropy of the chain segment, general polymers having aromatic groups such as polystyrene and polycarbonate show high values of Δn.

By using the model of the statistical segment approach introduced by Kuhn and Grun[2], the birefringence Δn is determined as,

$$\Delta n = \frac{2\pi}{9}\frac{(n+2)^2}{n}\frac{\rho N_A}{M_{seg}}\Delta\alpha\left[\frac{3\left\langle\cos^2\theta\right\rangle - 1}{2}\right] \tag{3}$$

Here, n, ρ and N_A are refractive index, density and Avogadro's number. M_{seg} and $\Delta\alpha$ are molecular weight and polarizability anisotropy of chain segment for the oriented polymers, and θ is the average angle between the segment and stretching direction. The bracket in the right hand of eq 3, [3<cos$^2\theta$>-1/2], represents the orientation function, F, and the following relation is obtained.

$$\Delta n = \Delta n^0 F \tag{4}$$

$$\Delta n^0 = \frac{2\pi}{9}\frac{(n+2)^2}{n}\frac{\rho N_A}{M_{seg}}\Delta\alpha$$

Δn^0 is an intrinsic birefringence for the anisotropic molecule perfectly orienting to the stretching direction.

Cellulose derivatives are expected as the eco-friendly materials for the various applications due to the biomass resources.[3-7] Particularly, cellulose esters (CEs) have been studied so far for the application to optical films due to their alternative properties such as heat resistance and transparency.[7-11] Retardation films, which are one of optical films, have to be improved for the optical devices such as stereo (3D) and organic electro-luminescence (OEL) displays. In addition, linear proportionality of birefringence against wavelength, which is called as "extraordinary wavelength dispersion", is required for high performance optical devices. For general polymers composed of single component, however, the birefringence decreases with wavelength (ordinary dispersion), since the strong absorption in ultraviolet region for polymers. In optical industries, the extraordinary dispersion is produced by blending with other component [12-16], laminating films [17], and copolymerization [18-20].

Recently, Yamaguchi et al. found that the cellulose acetate propionate (CAP, Fig.1) shows the extraordinary wavelength dispersion of birefringence without any extra components.[21] As shown in Fig.2, cellulose triacetate (CTA), which has only acetyl group as substitution group, exhibits ordinary dispersion. By compared the optical data of CTA, the extraordinary dispersion of CAP is originated from two different contributions from acetyl and propionyl groups as mentioned later in this paper. Furthermore, they explained the possibility to control the wavelength dependence by stretching conditions such as draw ratio. However, the mechanism is still unknown. If the stretching condition can control the wavelength dispersion of Δn, the new technique can be proposed to design an optical retardation film with ideal extraordinary dispersion. In this study, the wavelength dependence of birefringence for stretched CAP films at various conditions is investigated based on data of stress-strain curve, birefringence, thermal analysis and two-dimensional X-ray diffraction experiment.

[Figure 1]

[Figure 2]

EXPERIMENTAL

Samples

CAP sample was produced by Eastman Chemical Company (USA). The sample was obtained in a powdered state. The weight-average and number-average molecular weights (M_w and M_n) of CAP were 2.1×10^5 and 7.7×10^4, respectively, determined by a gel-permeation-chromatography (GPC, HLC-8020 Tosoh, Japan). Degrees of substitution for acetyl and propionyl groups per a pyranose unit of CAP are

0.19 and 2.58, respectively. In order to avoid the effect of water on physical properties, CAP powder was dried in vacuo at 80 ^{o}C for 2 hours prior to melt-compression. After kept in vacuum oven at room temperature at least for one day, the blend samples were compressed into sheets with a thickness of 200 μm at 200 ^{o}C for 5 min under 10 MPa by a compression-molding machine (Table-type-test press SA-303-I-S, Tester Sangyo, Japan) and were subsequently cooled down at 25 ^{o}C for 5 min.

In order to compare the crystallization effect on experimental results, cellulose triacetate (CTA) was also used. The sample characterization and preparation were reported in our previous paper.[9]

Measurements

A dynamic mechanical analysis (DMA) was carried out to measure tensile storage and loss moduli (E' and E'') at 10 Hz as a function of temperature by a tensile oscillatory rheometer (DVE-E4000, UBM, Japan) from 25 to 250 ^{o}C with a heating rate of 2 ^{o}C min^{-1}.

A hot-stretching test was performed at various conditions (draw ratio and strain rate) by using a tensile drawing machine (DVE-3, UBM, Japan). The stretching temperature (T_d) was chosen to be 163 and 215 ^{o}C for CAP and CTA, respectively, as explained in previous papers.[9, 21] For CAP, T_d was determined from the DMA data, where the storage modulus (E') is 10 MPa at 10 Hz. For CTA, T_d was selected from a plateau region of E' (> 100 MPa) beyond T_g in DMA data. The stretched films were immediately quenched by cold air blowing after stretching to avoid relaxation of molecular orientation.

The stretched samples were kept in a humidic chamber (IG420, Yamato, Japan)

at 25 ^{o}C and 50 %RH for one day in order to ignore the moisture effect on the optical properties as previously reported.[22] The birefringence was measured as a function of wavelength by using an optical birefringence analyzer (KOBRA-WPR, Oji Scientific Instruments, Japan). The detail of the optical system was explained in our previous paper.[21]

Thermal analysis was conducted by using a differential scanning calorimeter (DSC820, Mettler, USA) under a nitrogen atmosphere to avoid thermal-oxidative degradation. The sample of approximately 10 mg was put in an aluminum pan. The first heating curve was recorded at a heating rate of 10 ^{o}C min^{-1}.

In order to investigate an anisotropic crystalline structure, two dimensional wide-angle XRD patterns were recorded using a graphite monochromatized CuKa radiation beam focused via a 0.3 mm pinhole collimator with a flat 20 × 20 cm^2 imaging plate (IP) detector of 1900 × 1900 pixels (R-AXIS IIc, Rigaku, Japan). A small piece of the sample with edge sizes less than 1 mm was mounted with the sample-IP distance of 10 cm. The exposure was performed with 7 min a shot in a geometrical condition by directing the X-ray beam in normal direction (ND) to the film plane (MD-TD).

RESULTS and DISCUSSION

Mechanical property of CAP film

Temperature dependence of E' and E'' for CAP is shown in Fig.3. The α relaxation peak of E'' is observed around at 150 ^{o}C, which corresponds to the glass transition temperature (T_g). No extra peak is observed below T_g, suggesting that a local motion of CAP chain including ester groups is not active at a glassy state. Moreover, E' decreases from 10^9 to 10^6 Pa in the vicinity of T_g, and does not show a

plateau region beyond T_g. Contrary, CTA has the plateau value of 10^8 Pa in E' due to the cross-link effect of micro-crystallites.[23] By considering the result of CTA, no plateau region beyond T_g in Fig.3 indicates that the degree of crystallization for unstretched CAP film is zero or negligibly small. As discussed later, a DSC curve of a neat CAP film shows no melting peak, suggesting that unstretched CAP is amorphous before stretching.

[Figure 3]

Hot-stretching behaviors of CAP film at various conditions

To generate the birefringence (Δn), the compressed CAP film was stretched at various draw ratios (DRs) and strain rates (SRs). Fig.4 (A) shows the stress-strain (S-S) curves of CAP films during uni-axially stretching at 0.014 s^{-1} of SR. The stress value monotonically increases with the tensile strain, meaning that the chain orientation of CAP becomes stronger. At the small region of DR (< 2.0), the S-S curve became a convex upward due to the stress-relaxation originated from the orientation relaxation. On the other hand, the strain-hardening is observed beyond 2.5 of DR. This behavior usually appears for semi-crystalline and rubbery polymers because of the limit on chain extensibility between entanglements or cross-link points.[24] Therefore, the strain-hardening behavior indicates that the crystallization of CAP is induced by the hot-stretching.

[Figure 4]

Fig.4 (B) shows the S-S curves of CAP at different strain rates. The tensile stress increases with strain rate. According to the Boltzmann superposition principle, the tensile stress at time *t* during a uniaxial stretching, $\sigma(t)$ is given by,

$$\sigma(t) = \int_{-\infty}^{t} E(t-s)\dot{e}(s)\mathrm{d}s \tag{5}$$

Here, $E(t)$ is Young's relaxation modulus and $\dot{e}$ is a tensile strain rate. From this equation, it is obvious that the high strain rate enhances the tensile stress as shown in Fig.4 (B). More precisely, for semi-crystalline polymers such as CAP, the stress of semi-crystalline polymers is originated from chain orientation, the degree of crystallinity, and the crystal orientation.

The strain hardening behavior is observed in all S-S curves in Fig.4 (B). The stress rise became small at lower SR, indicating that the crystallization of CAP is dependent upon the stretching speed. This result is discussed later with results of thermal analysis and X-ray diffraction experiments.

Birefringence of CAP at various draw ratios and strain rates

The birefringence of stretched films is proportional to the degree of chain orientation as represented in eq.4. Previous section mentioned that both larger DR and higher SR generate the stronger orientation of CAP chain. Therefore, it is predicted that the birefringence increases with increasing DR / SR.

Fig.5 (A) shows the wavelength dependence of birefringence (Δn) for stretched CAP film at various DRs. Δn is positive and increases with DR. The wavelength dependence is extraordinary dispersion: Δn increases with wavelength. As shown in

Fig.5 (B), the wavelength dependence becomes stronger at larger DRs. The change in wavelength dependence for CAP is not observed in other optical polymers such as poly(methyl methacrylate) and poly carbonate.

[Figure 5]

In general, the birefringence (Δn) is determined as the product of the intrinsic birefringence (Δn^0) and the orientation function (F) as represented by eq.4. Therefore, the wavelength (λ) dependence of Δn is the same with that of Δn^0 as given by,

$$\frac{\Delta n(\lambda)}{\Delta n(\lambda_0)} = \frac{\Delta n^0(\lambda)}{\Delta n^0(\lambda_0)} = const. \quad (6)$$

Here, λ_0 is the reference wavelength, which is 589 nm in Fig.5 (B). The eq.6 cannot explain the change of wavelength dependence.

From the comparison of experimental data for various cellulose esters, Yamaguchi et al.[21] suggested that the wavelength dependence of birefringence for cellulose esters such as CAP is affected by ester groups. Since the birefringence is a difference of two refractive indices (n), the wavelength dependence of birefringence is reflected from that of n. As shown in Fig.S1, CAP and cellulose triacetate (CTP) show weaker wavelength dependence of n than CTA, suggesting that the acetyl group provides the stronger wavelength dependence of birefringence than the propionyl, as concluded in the paper. Since CAP has acetyl (ac) and propionyl (pr) groups, the birefringence (Δn_{CAP}) is provided by the sum of three components (a main chain and two ester groups) as represented by,

$$\Delta n(\lambda) = \Delta n_{\mathrm{main}}(\lambda) + \Delta n_{\mathrm{ac}}(\lambda) + \Delta n_{\mathrm{pr}}(\lambda) \quad (7)$$

Here, Δn_{main} is the birefringence from a pyranose ring on the main-chain. The paper explained that the acetyl group contributes negative birefringence and strong wavelength dependence of ordinary dispersion while the propionyl group exhibits positive and weak wavelength dependence. Since the contribution of the pyranose ring to birefringence is negligibly small, the total birefringence of CAP becomes positive and extraordinary dispersion as the sum of two components from acetyl and propionyl groups as shown in Fig.6.

[Figure 6]

Based on their idea, the change of wavelength dependence can be explained by the contributions of acetyl and propionyl groups to birefringence. As shown in Fig.5 (B), the wavelength dependence was stronger with increasing DR, meaning that the contribution of acetyl group is larger at the high DR. The difference in two ester contributions is discussed with the result of a thermal experiment in the next section.

In order to discuss the effect of strain rate (SR), Fig.7 (A) compares the birefringence data as the function of wavelength for CAP films stretched with various SRs. The highest birefringence value at 0.05 s^{-1} of SR was observed although the tensile stress monotonically increased with SR as represented in Fig.4 (B). Moreover, Fig.7 (B) reveals that the wavelength dependence of birefringence is dependent on SR: the gradient of birefringence against wavelength becomes stronger with higher SR.

This result is also explained by the contributions of two ester groups. The larger gradient at higher SR is attributed to the larger contribution of acetyl group, which has stronger wavelength dependence.

[Figure 7]

Fig.8 shows relation between the birefringence (Δn) at 633 nm and tensile stress (σ) for stretched CAP films. The solid line represents the estimated value by assuming the SOR represented in eq.2 with $C = 2.5 \times 10^{-9}$ Pa^{-1}, which was reported by Maeda and Inoue.[25] Large deviations between the experimental and estimated values are observed at a higher stress region (> 1 MPa). Moreover, as shown in Fig.8 (B) for the samples with various SRs, the highest value of Δn is observed at 0.03 - 0.05 s^{-1} of SR. The maximum point is related to the degree of crystallinity (no the stress value) as explained in the final part.

[Figure 8]

Stretching-induced crystallization of CAP

In order to confirm the crystallization of CAP during hot-stretching at various conditions, DSC measurements were performed. Fig.9 shows the DSC curves of stretched CAP films at various DRs (A) and SRs (B). All data show endothermic peak around at 70 ^{o}C due to a small content of water (< 2 wt%).[22] In Fig.9 (A), an endothermic peak at 160 - 170 ^{o}C, which reflects the crystal melting, appears for stretched films with higher DR (> 2.0), indicating that the stretched-induced

crystallization of CAP takes place during the hot-stretching. The threshold of DR (= 2.0) corresponds to the rise of the S-S curve in Fig.4 (A), meaning that the strain-hardening is associated with the crystallization.

[Figure 9]

The difference between the melting point (T_m) and T_g for CAP (140 / 160-170 ^oC) is relatively smaller than that for other cellulose esters, *e.g.*, 190 / 290 ^oC and 133 / 234 ^oC, for CTA and cellulose tripropionate (CTP), respectively. [26] The small difference for CAP can be explained by two factors; (i) decrease of T_m by a copolymerization effect (a steric hindrance by propionyl group), and (ii) the small change of T_g from CTP. (i) CAP is one of copolymers, which is composed of cellulose acetate and cellulose propionate. According to Flory's theory [27], T_m of random copolymers is depressed with other monomer content as given by,

$$1/T_m - 1/T_m^0 = -(R/\Delta H)\ln p \quad (8)$$

Here, p and T_m^0 are the sequence perpetuation probability and the melting point of homopolymer. The depression of T_m is also understood by the disordering of the crystal for the cellulose ester due to the two ester groups. Therefore, T_m of CAP is lower than that of CTP (234 ^oC). (ii) In contrast, T_g of copolymers can be estimated by the Fox equation. [28]

$$1/T_g = w_1/T_{g,1} + w_2/T_{g,2} \quad (9)$$

where w is the weight fraction. Since the main ester group of CAP is propionyl, T_g is almost similar to that of CTP (133 ^oC). As the result of two factors (i) and (ii), the difference of T_g and T_m of CAP become small.

Since the stretching temperature (163 ^oC) is close to the melting temperature determined from the DSC data, the crystallization of CAP is possible during the hot-stretching. Heat of fusion (ΔH) and melting point (T_m) are plotted against DR in Fig.10(A). With increasing DR, ΔH becomes larger and T_m slightly shifts to higher, meaning that the crystallinity and the crystal size are improved during the hot-stretching. The result of ΔH is qualitatively similar to the stress and birefringence data, in which both values increased with DR.

[Figure 10]

The DSC curves of stretched films at various SRs (DR = 2.0) are represented in Fig.9(B). All samples show the melting peak at 160 – 170 ^oC. ΔH and T_m were estimated from the DSC curves as plotted in Fig.10(B). At lower SRs (0.003 – 0.05 s^{-1}), T_m decreases and ΔH increases with SR, suggesting that the larger amount of smaller crystal forms at higher SRs. At higher SRs (0.05 – 0.2 s^{-1}), T_m shows a plateau value while ΔH is decreasing, representing that the crystal size reaches a constant and the degree of crystallinity decreases with SR. Therefore, ΔH showed a maximum at 0.05 s^{-1} due to the slower crystallization rate than the stretching rate. The birefringence data also exhibited the maximum value at 0.05 s^{-1}, although the stress data

did not (it increased with SR). By considering DR and SR dependences, ΔH should be associated with birefringence (not stress). Instead, the increase of stress with SR in Fig.4(B) enhances the orientations of both amorphous chain and crystal for CAP.

In order to confirm the orientation of CAP crystal, 2D wide-angle X-ray diffraction (XRD) data is examined. Fig.11 shows 2D XRD patterns for CAP (DR = 4.0) and CTA (DR = 1.5) stretched films. The X-ray beam was inserted into the samples through the film plane composed of machine and transversal directions (MD and TD). In the XRD data for CAP, two weak spots at 2θ = 7.0 ^{o} (inner ring) are observed on the equatorial direction (MD). For CTA, on the other hand, the strong anisotropic pattern is obtained even for smaller DR. Comparison of the two data suggests that the crystal orientation of CAP is lower than that of CTA.

[Figure 11]

In order to estimate the crystal orientations, the 2D XRD profiles are evaluated as follows. Fig.12 (A) compares 2θ profiles of XRD for CAP and CTA. The peaks at 2θ = 8.5 ^{o} and 17.0 ^{o} for CTA are assigned to be (110) and (210) reflections from the CTA crystal, respectively.[29] Since the broader peak at 2θ = 7.0 ^{o} for CAP may contain two or more than three reflections, the peak reflection cannot be identified. However, we think that the main reflection is (110), and the crystal orientation f_c for CTA and CAP is evaluated by using a following equation.

$$< \cos^2 \phi >= \frac{\int_0^{\pi/2} I(\phi) \cos^2 \phi \sin \phi \mathrm{d}\phi}{\int_0^{\pi/2} I(\phi) \sin \phi \mathrm{d}\phi} \tag{10}$$

$$f_c = \frac{3 < \cos^2 \phi > -1}{2} \quad (11)$$

Here, I is the peak intensity and ϕ is the azimuthal angle. Fig.12 (B) shows the peak profiles against the azimuthal angle for CAP and CTA. Both curves represent the peaks at 90 ^{o}, meaning the crystal orientation to MD. By using eqs.10 and 11, the values of f_c for CAP and CTA are estimated to be 0.42 and 0.79, respectively. Therefore, the crystal orientation of CAP is lower than that of CTA even though the DR is larger.

[Figure 12]

Effect of crystal orientation on birefringence

The previous sections discussed the effects of hot-stretching on birefringence and crystallization behavior. It was concluded that the wavelength dependence of birefringence is dependent on the stretching conditions such as DR and SR. The thermal and X-ray experiments revealed that the hot-stretching induces crystallization and its orientation. Based on the size difference of ester groups, it is speculated that the acetyl group is more confined in the crystal of CAP than the propionyl group. Since the crystal relaxation is slower than the amorphous, the acetyl group has lower mobility than the propionyl.

In Fig.8, the birefringence showed the maximum at 0.05 s^{-1} of SR while it monotonically increased with DR. Since ΔH exhibited the highest value at the same SR, the correlation between birefringence and crystallinity is suggested. For amorphous polymers such as polystyrene and polycarbonate [30], the birefringence

monotonically increases with SRs. On the other hand, for semi-crystalline polymers such as poly(ethylene terephthalate), the birefringence is the sum of two components, amorphous and crystalline birefringences. [31]

$$\Delta n = \Delta n_a^0 (1 - X_c) F_a + \Delta n_c^0 X_c F_c \tag{12}$$

Here, X_c is the degree of crystallinity. The two birefringences are proportional to orientation functions, F_a and F_c. Since the relaxation time of amorphous orientation is much shorter than that of crystalline orientation, the crystalline component relatively contributes to the optical anisotropy rather than the amorphous one. Therefore, it is reasonable that X_c ($\propto \Delta H$) showed the same dependence on DR and SR with Δn.

As previously mentioned, the stretched film with high DR and SR exhibited strong wavelength dependence of birefringence. It indicates that, in the stretched films at larger DR, the acetyl group, which contributes the strong wavelength dispersion, more highly orients than the propionyl. Although a dichroic Fourier-transform infrared (FT-IR) spectroscopy is useful to evaluate the chain orientation, it enable to be applied for the ester orientations of CAP because the IR absorption peaks such as C=O and C-H in acetyl and propiony groups are overlapped. Therefore, the speculation of two ester orientations is deduced from only the wavelength dependence of birefringence in this study.

As already explained in Figs.5(B) and 7(B), the wavelength dependence of Δn became stronger with increasing DR and SR. The degree of crystallinity ($\propto \Delta H$) reached the constant value at higher SR ($> 0.05\ s^{-1}$) while it increased with DR (> 2.0) in Fig.10. Since the DR and SR dependences of ΔH are not consistent with the stress

data, the effect of crystallization on wavelength dependence of birefringence should be discussed.

Since the pyranose ring contributes no birefringence, eq.7 is rewritten as,

$$\Delta n_{\mathrm{CAP}} = \Delta n^0_{\mathrm{ac}} \phi_{\mathrm{ac}} f_{\mathrm{ac}} + \Delta n^0_{\mathrm{pr}} \phi_{\mathrm{pr}} f_{\mathrm{pr}} \tag{13}$$

Here, Δn^0, ϕ and f are intrinsic birefringence, volume fraction, the degree of orientation for ester group. Δn^0 and ϕ are independent of the stretching conditions. For the amorphous state, since the orientation of ester groups is determined by the chain orientation, the ratio of $f_{\mathrm{ac}}/f_{\mathrm{pr}}$ is expected to be a constant. After crystallization induced by stretching, however, the orientation ratio may be changed by two factors; the degree of crystallinity and the crystal orientation. The acetyl group in CAP is more tightly confined in the crystal compared with the propionyl. The crystallization of CAP is induced by the stretching, and the crystal orientation becomes stronger at larger DR or higher SR. As the result, the acetyl orientation is improved with increasing the degree of crystallization and the crystal orientation. Especially, at higher region of SR ($> 0.05\ s^{-1}$), although the crystallinity was a constant, the acetyl orientation is enhanced with the crystal orientation.

Conclusions

In this study, the effect of birefringence for cellulose acetate propionate (CAP) on stretching conditions is investigated from the results of stress-strain curve, birefringence, DSC, and X-ray diffraction. Hot-stretching test was performed at 163 ^{o}C ($> T_g$) with various draw ratios and strain rates. Although the CAP is

amorphous after preparing as a sample film using a compression molding, stress-strain curves showed the rubber-like strain-hardening behavior at higher draw ratio (> 2.0). The result suggested that a strain-induced crystallization occurred.

Birefringence of stretched CAP films exhibited extraordinary wavelength dispersion: birefringence increases with increasing wavelength. In our previous paper, the wavelength dependence has been explained with the two contributions from acetyl and propionyl groups. In the present work, the experimental data represented that the wavelength dependence was changed with increasing draw ratio and strain rate, suggesting that the ratio of two ester contributions was not constant against stretching conditions.

Results of DSC and two-dimensional XRD experiments clarified the strain-induced crystallization and orientation during the hot-stretching test. The 2D XRD pattern for stretched CAP (DR = 4.0) showed two weak spots on the equatorial direction. The 2D-XRD profile has been observed for stretched cellulose triacetate (CTA) although the peak strength is stronger. The azimuthal analysis suggested that the CAP crystal oriented to the stretching direction as well as amorphous chain. Considering with data of stretching test and birefringence measurement, we concluded that the change in wavelength dispersion of birefringence for CAP was originated from stronger contribution of acetyl group than propionyl. The conclusion is reasonable because acetyl group is tightly confined to a pyranose ring in main chain rather than propionyl.

ACKNOWLEDGEMENTS

We gratefully acknowledge financial support from a Grant-in-Aid for Young

1 Scientists B (25870268) by the Japan Society for the Promotion of Science.

2

REFERENCES

1. Doi M and Edwards SF. The Theory of Polymer Dynamics. New York: Oxford University Press, 1986.
2. Wilkes GL and Stein RS. Structure and Properties of Oriented Polymers. Chapt. London: Chapman & Hall, 1997. pp. 44-141.
3. Edgar KJ, Buchanan CM, Debenham JS, Rundquist PA, Seiler BD, Shelton MC, and Tindall D. *Prog. Polym. Sci.* 2001;26:1605-1688.
4. Kondo T, Sawatari C, Manley RS, and Gray DG. *Macromolecules* 1994;27:210-215.
5. Krasovskii AN, Plodistyi AB, and Polyakov DN. *Russ. J. Appl. Chem.* 1996;69:1048-1054.
6. Heinze T, Dicke R, Koschella A, Kull AH, Klohr EA, and Koch W. *Macromol. Chem. Phys.* 2000;201:627-631.
7. Sata H, Murayama M, and Shimamoto S. Properties and applications of cellulose triacetate film. Heidelberg, Germany: Wiley-VCH, 2003.
8. Ilharco LM and de Barros RB. *Langmuir* 2000;16:9331-9337.
9. Songsurang K, Miyagawa A, Abd Manaf ME, Phulkerd P, Nobukawa S, and Yamaguchi M. *Cellulose* 2012;20:83-96.
10. Hishikawa Y, Togawa E, and Kondo T. *Cellulose* 2010;17:539-545.
11. Yamaguchi M, Abd Manaf ME, Songsurang K, and Nobukawa S. *Cellulose* 2012;19:601-613.
12. Saito H and Inoue T. *J. Poly. Sci. Part-B Poly. Phys.* 1987;25:1629-1636.
13. Uchiyama A and Yatabe T. *Japan J. App. Phys. Part-1* 2003;42:3503-3507.
14. Tagaya A, Iwata S, Kawanami E, Tsukahara H, and Koike Y. *App. Opt.* 2001;40:3677-3683.
15. Tagaya A, Ohkita H, Harada T, Ishibashi K, and Koike Y. *Macromolecules* 2006;39:3019-3023.
16. Abd Manaf ME, Tsuji M, Shiroyama Y, and Yamaguchi M. *Macromolecules* 2011;44:3942-3949.
17. Cho CK, Kim JD, Cho K, Park CE, Lee SW, and Ree M. *J. Adh. Sci. Tech.* 2000;14:1131-1143.
18. Iwasaki S, Satoh Z, Shafiee H, Tagaya A, and Koike Y. *Polymer* 2012;53:3287-3296.
19. Uchiyama A, Ono Y, Ikeda Y, Shuto H, and Yahata K. *Polym. J.* 2012;44:995-1008.
20. Cimrova V, Neher D, Kostromine S, and Bieringer T. *Macromolecules*

1999;32:8496-8503.
21. Yamaguchi M, Okada K, Abd Manaf ME, Shiroyama Y, Iwasaki T, and Okamoto K. *Macromolecules* 2009;42:9034-9040.
22. Abd Manaf ME, Tsuji M, Nobukawa S, and Yamaguchi M. *Polymers* 2011;3:955-966.
23. Nobukawa S, Enomoto-Rogers Y, Shimada H, Iwata T, and Yamaguchi M. *Cellulose* 2015;22:3003-3012.
24. Haward RN. 1993;26:5860-5869.
25. Maeda A and Inoue T. *Nihon Reoroji Gakkaishi* 2011;39:159-163.
26. Klarman AF, Galanti AV, and Sperling LH. *J. Polym. Sci. Part a-2, Polym. Phys.* 1969;7:1513-1523.
27. Richardson MJ, Flory PJ, and Jackson JB. *Polymer* 1963;4:221-236.
28. Stroble GR. The Physics of Polymers. Verlag Berlin Heidelberg: Springer, 2007.
29. Kono H, Numata Y, Nagai N, Erata T, and Takai M. *J. Polym. Sci. Pol. Chem.* 1999;37:4100-4107.
30. Luap C, Muller C, Schweizer T, and Venerus DC. *Rheo. Acta* 2005;45:83-91.
31. Dumbleton JH. *J. Polym. Sci. Part A-2, Polym. Phys.* 1968;6:795-800.

Figure captions

Figure 1. Chemical structure of cellulose acetate propionate (CAP).

Figure 2. Wavelength dependence of stretched CAP and CTA films.

Figure 3. Dynamic mechanical properties for (A) CAP and (B) CTA. Applied frequency is 10 Hz, and heating rate is 2 ^{o}C min^{-1}.

Figure 4. Stress-strain curves of CAP film during stretching at 163 ^{o}C with various draw ratios and strain rates.

Figure 5. (A) Wavelength dependence of birefringence for stretched CAP films at different draw ratios with the strain rate of 0.014 s^{-1}. (B) Comparison of wavelength dependence of normalized birefringence.

Figure 6. Schematic illustration for extraordinary wavelength dispersion of CAP. Acetyl and propionyl groups contribute negative/strong wavelength dependence and positive/weak dependence. The total birefringence shows extraordinary dispersion as the sum of two components.

Figure 7. (A) Wavelength dependence of birefringence for stretched CAP films at various strain rates. (B) Comparison of wavelength dependence of normalized birefringence.

Figure 8. Stress-optical relation of CAP films at various draw ratio and strain rate. The solid line represents linear relation using the literature value.[25] Labels are explained for (A) draw ratio (DR) and (B) strain rate (SR). (B) is an extended view to distinguish the plots more clearly.

Figure 9. DSC curves of stretched CAP films at various (A) draw ratios and (B) strain rates. Heating scan rate is 10 ^{o}C min^{-1}.

Figure 10. Heat of fusion (ΔH) and melting temperature (T_m) analyzed from data in Fig.9.

Figure 11. 2D-XRD patterns of stretched (A) CAP and (B) CTA films in MD-TD plane.

Figure 12. (A) XRD profiles against 2θ for stretched CAP and CTA films. (B) Peak profiles of the stretched films against azimuthal angle. The reflection peaks are observed at 7.0 and 8.5 ^{o} for CAP and CTA, respectively.

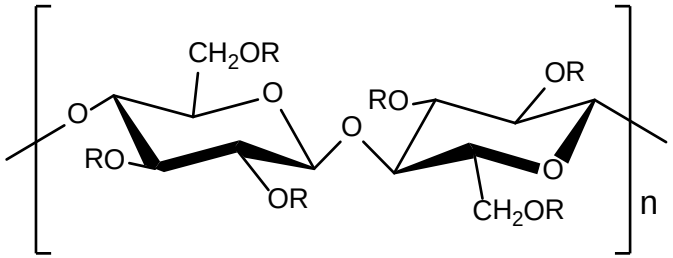

R = $COCH_3$ (acetyl)
= $COCH_2CH_3$ (propionyl)

Nobukawa et al.

Figure 1

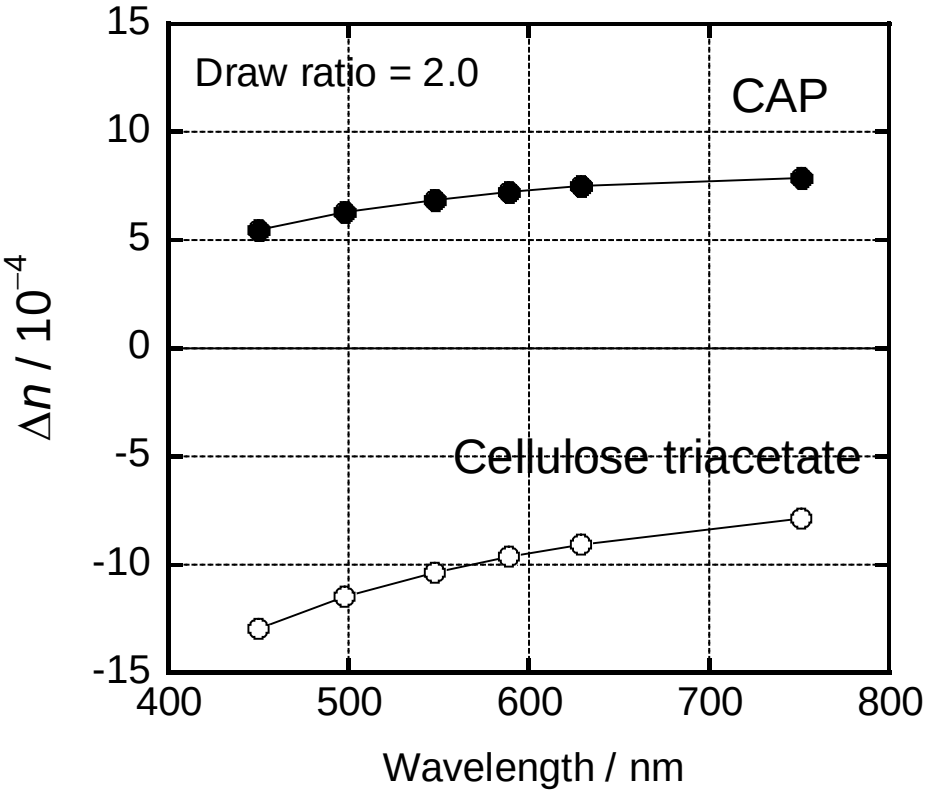

Nobukawa et al.

Figure 2

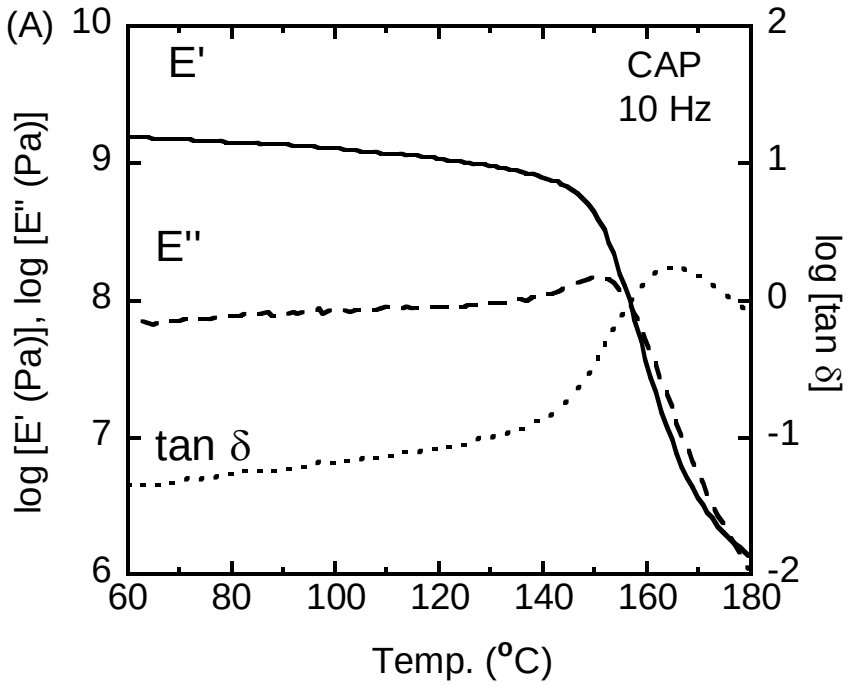

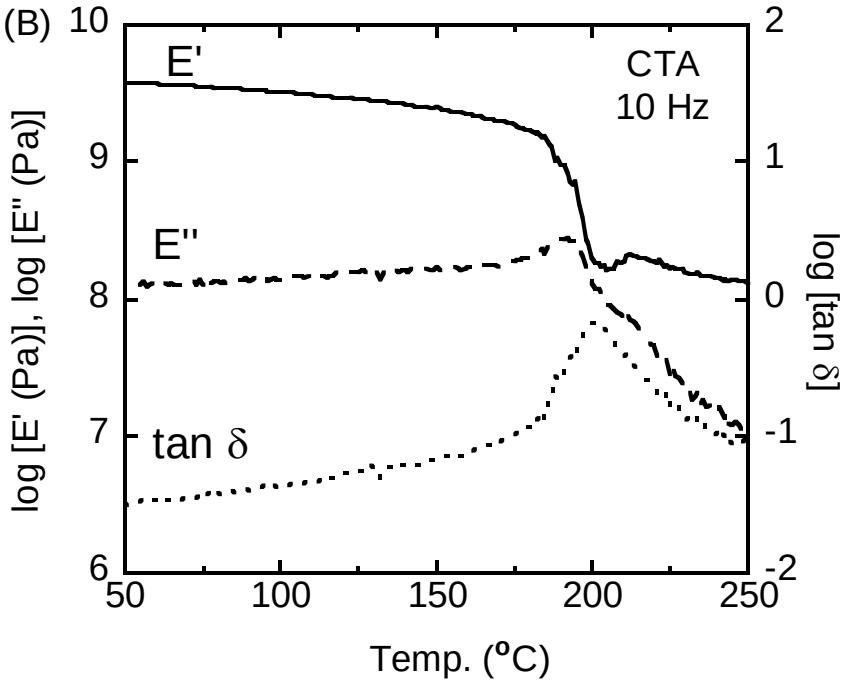

Nobukawa et al.

Figure 3

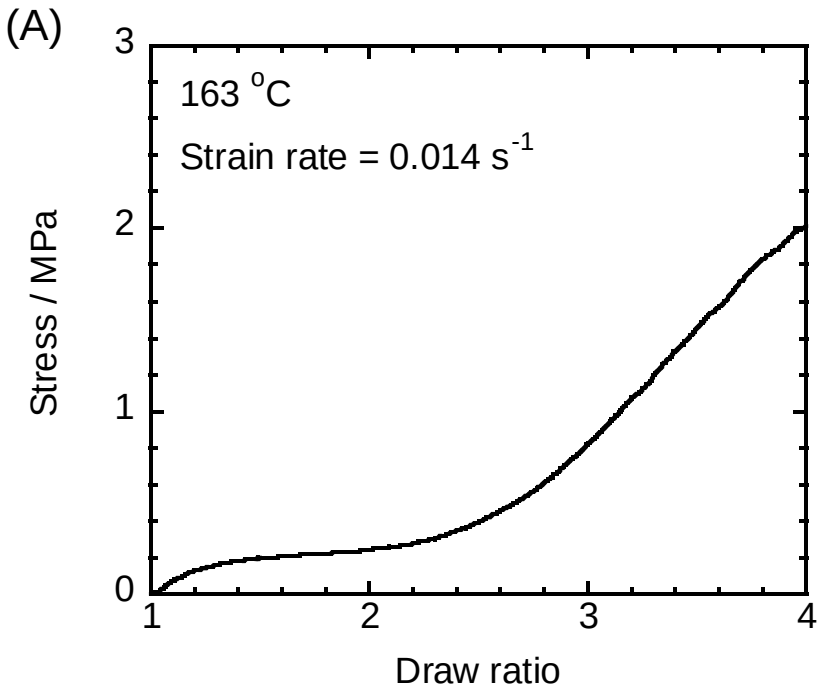

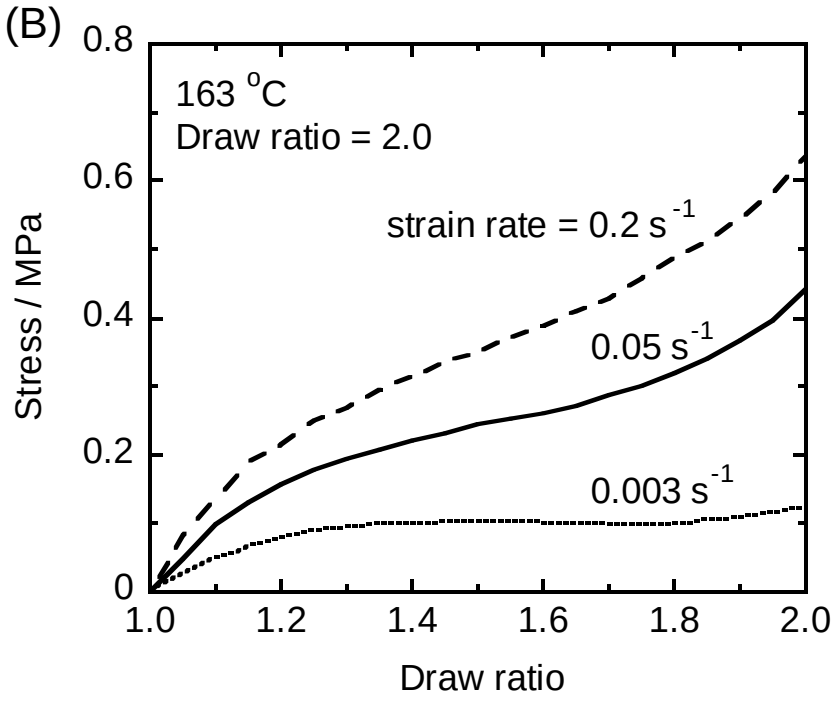

Nobukawa et al.

Figure 4

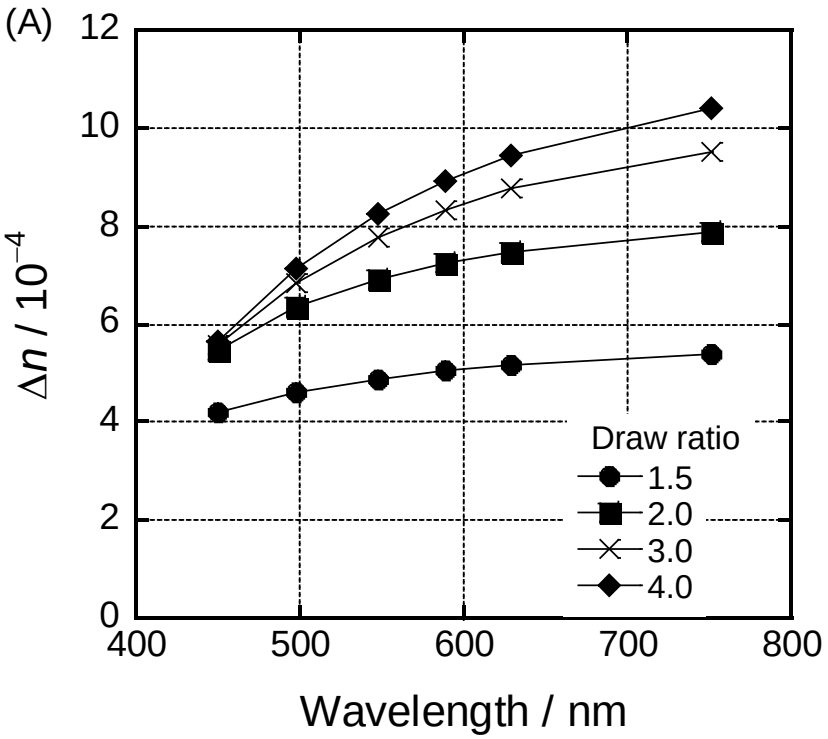

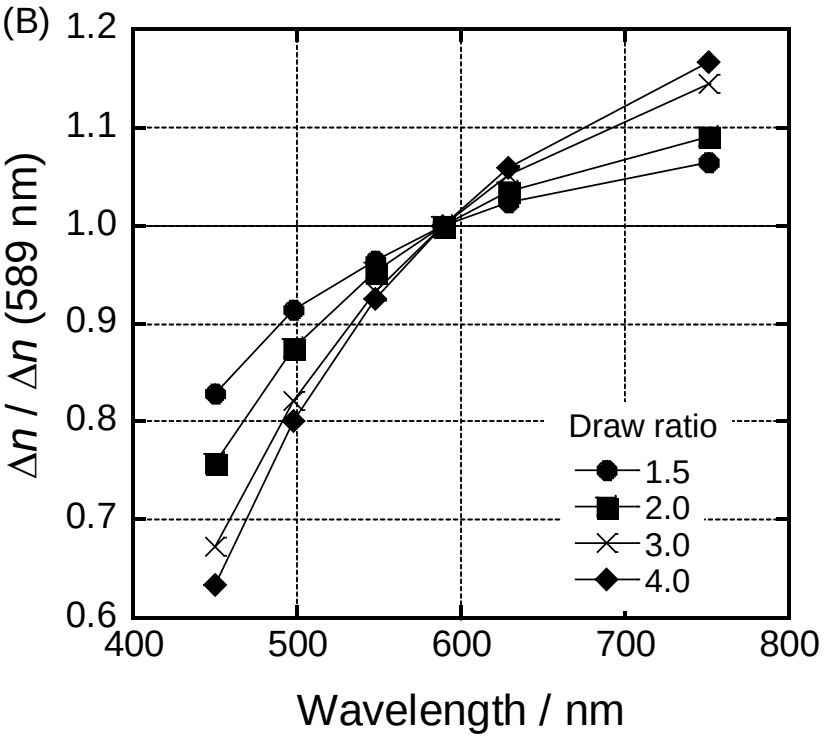

Nobukawa et al.

Figure 5

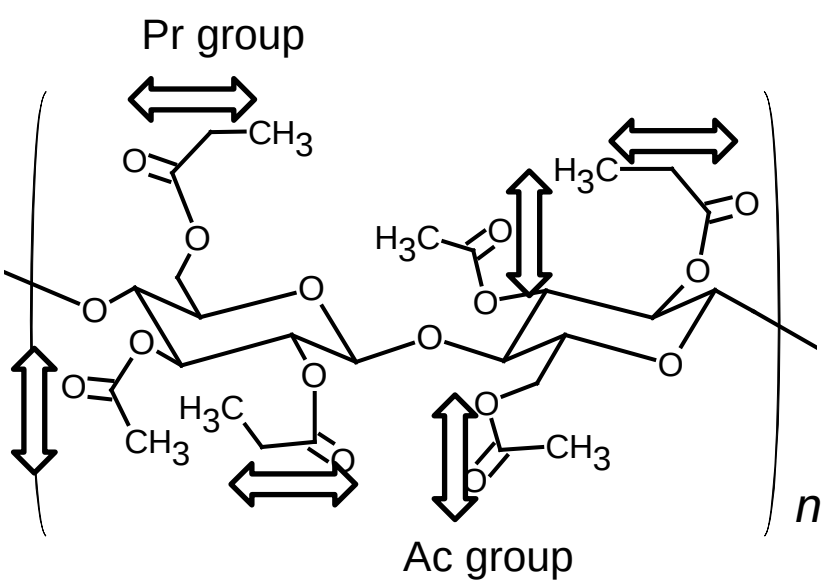

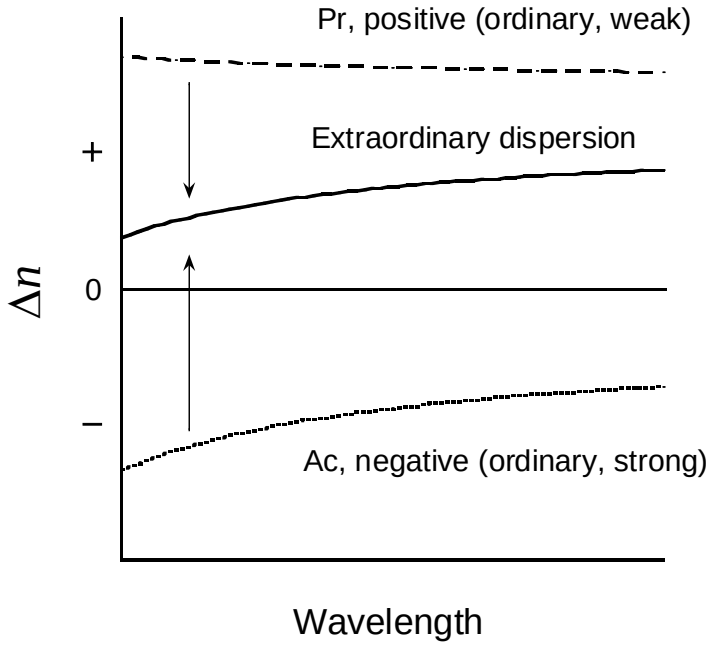

Nobukawa et al.

Figure 6

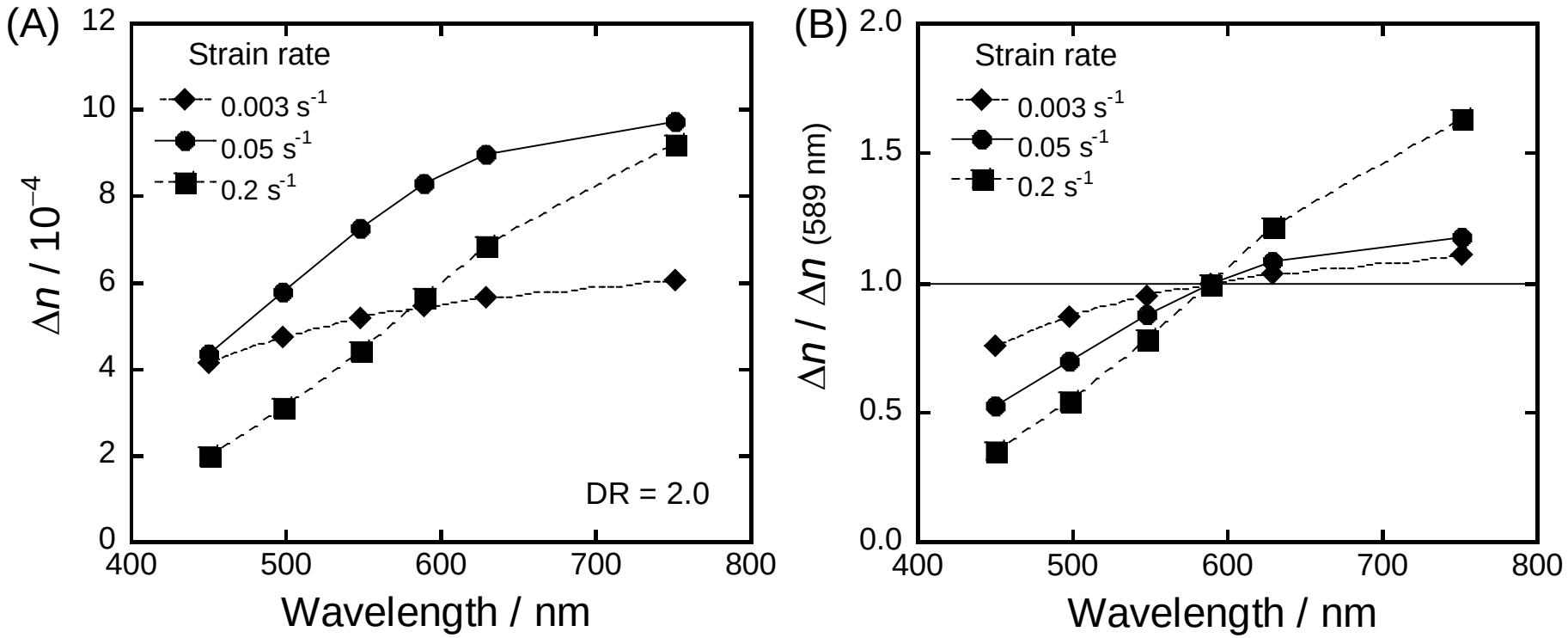

Nobukawa et al.

Figure 7

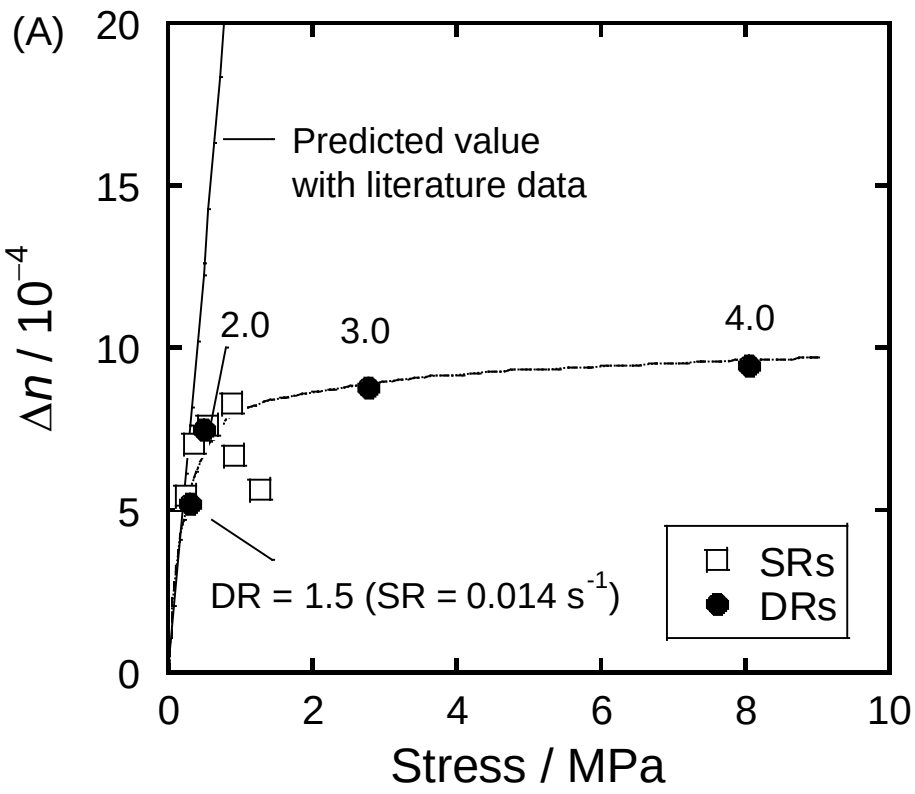

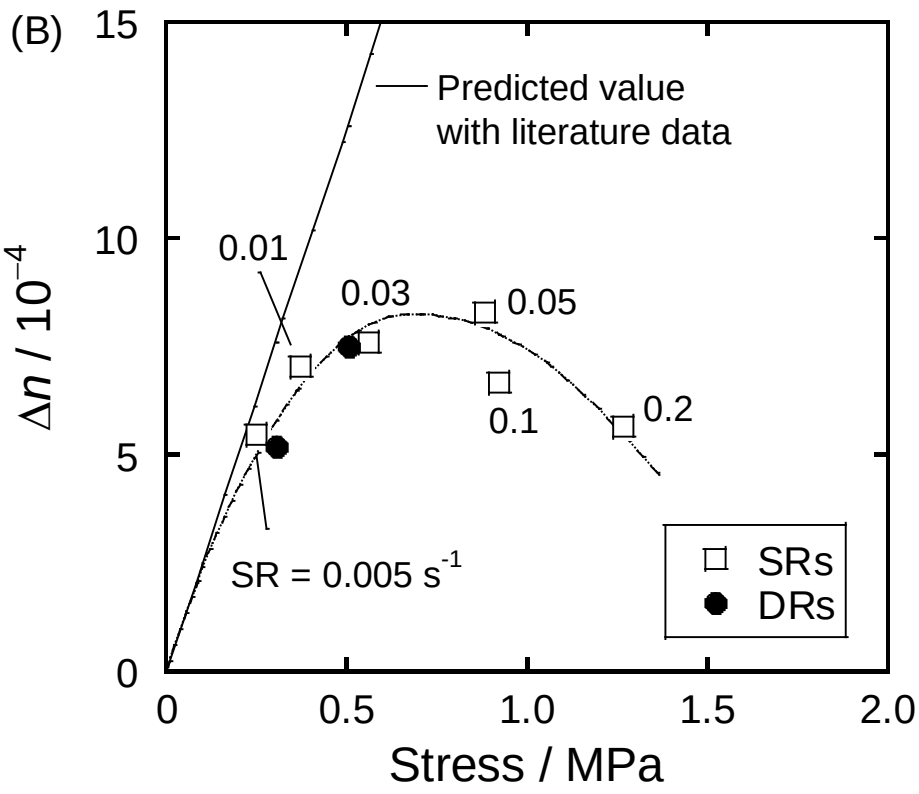

Nobukawa et al.

Figure 8

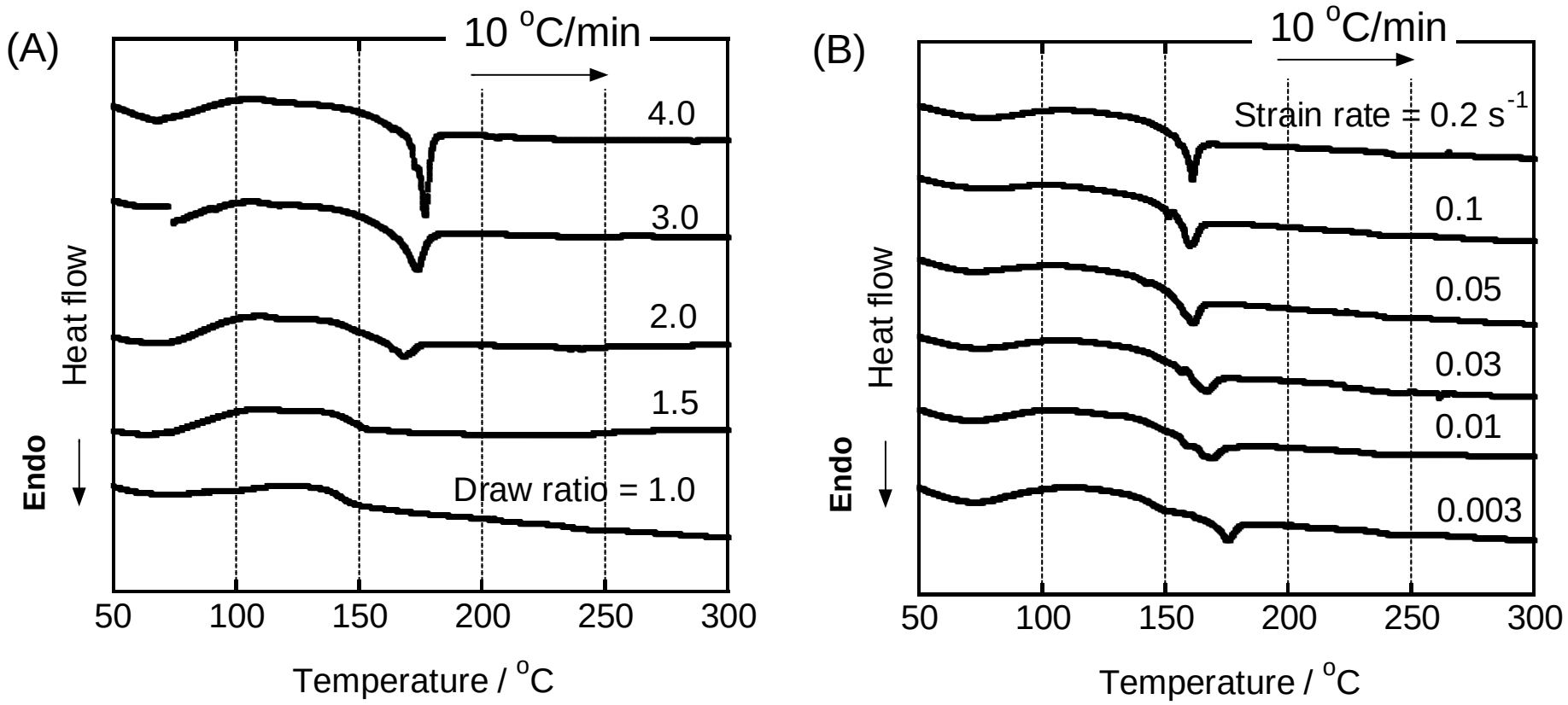

Nobukawa et al.

Figure 9

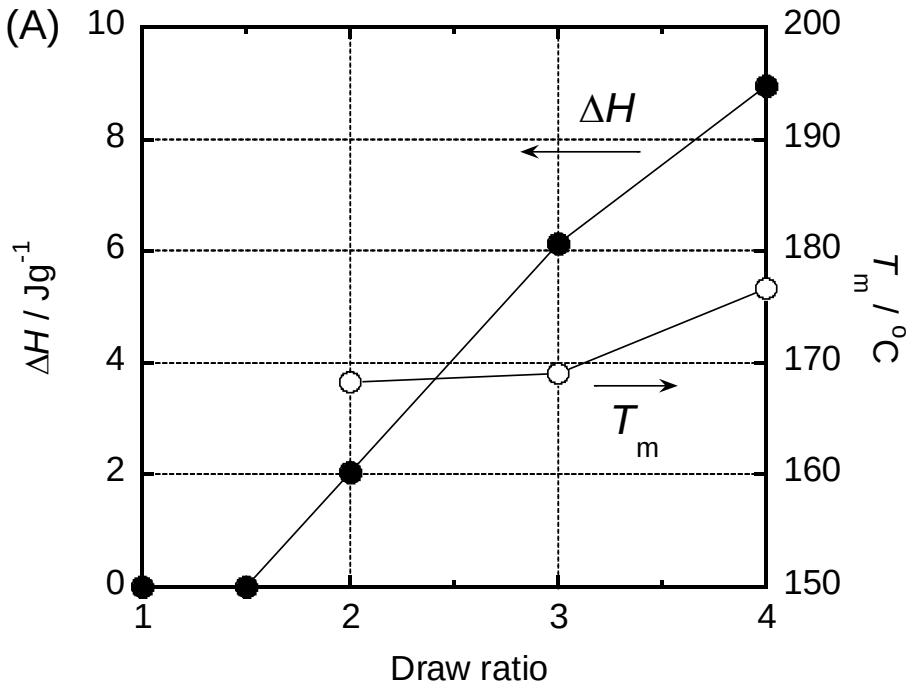

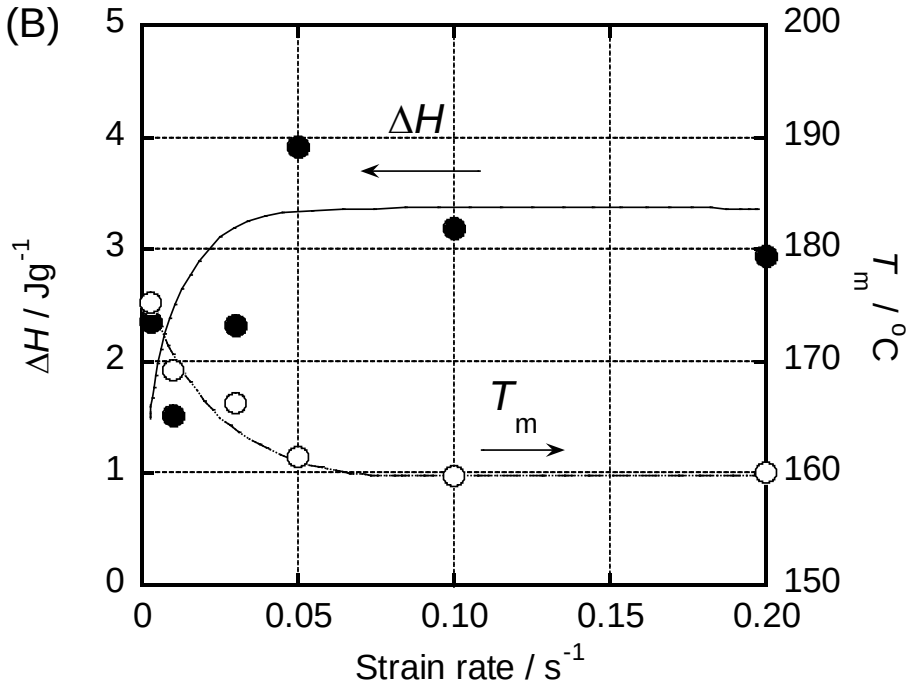

Nobukawa et al.

Figure 10

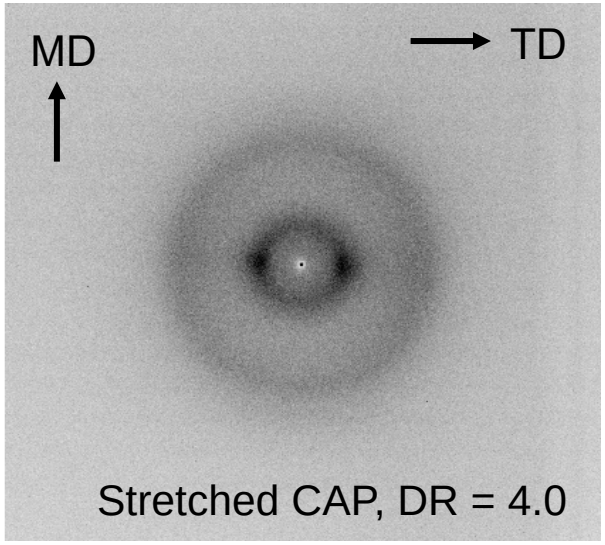

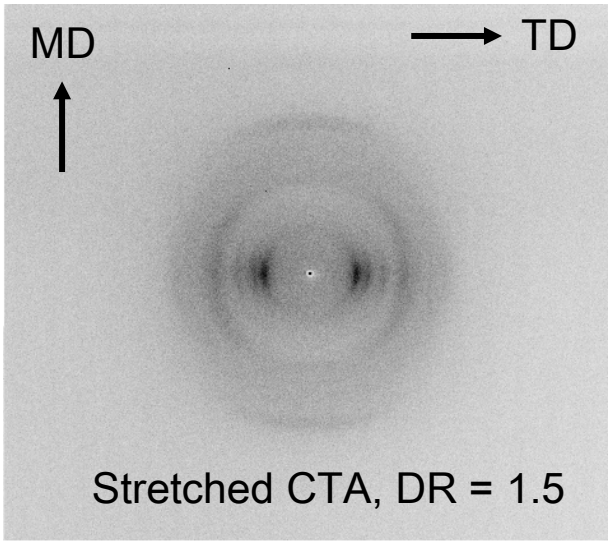

Nobukawa et al.

Figure 11

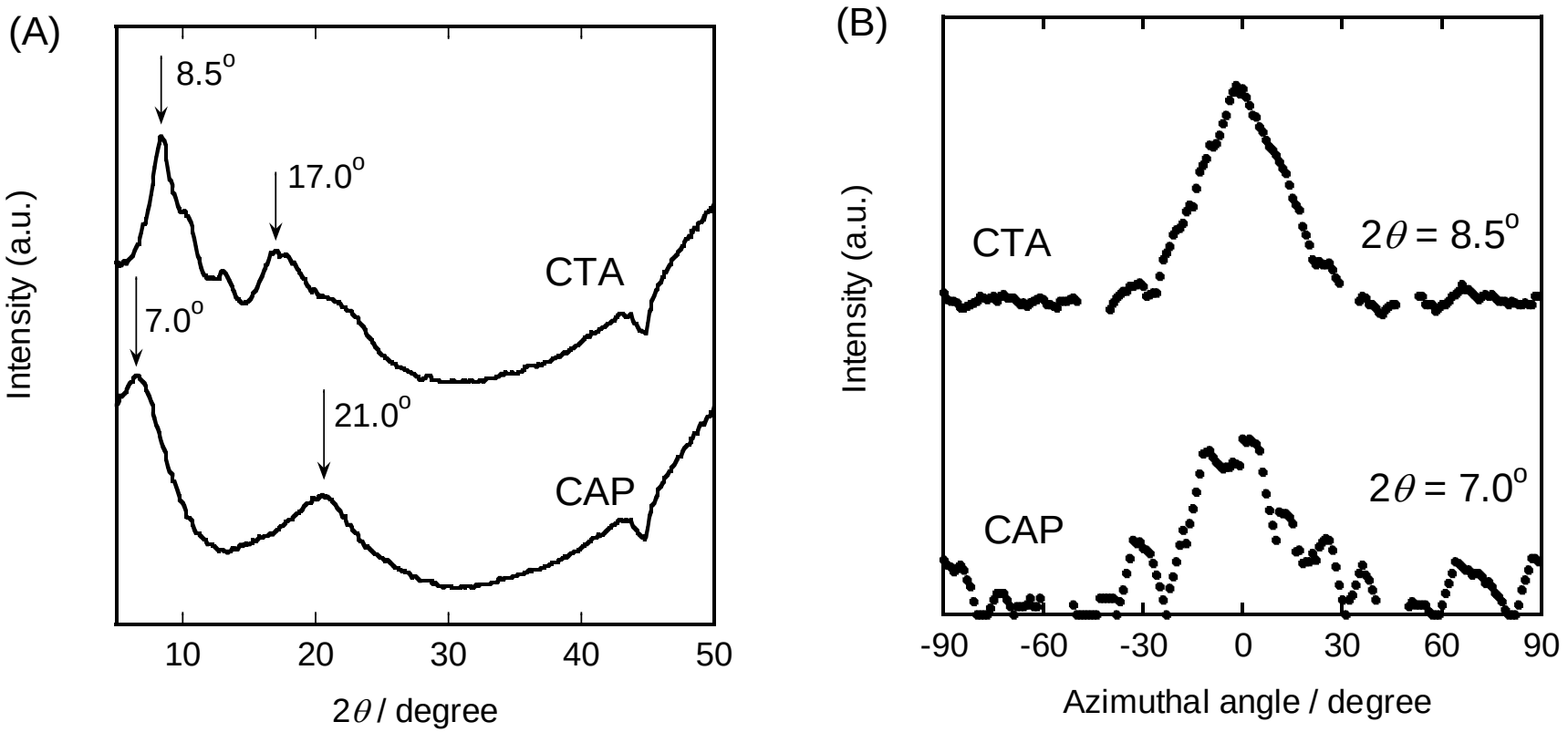

Nobukawa et al.

Figure 12